Wedge Diffraction as an Instance of Radiative Shielding

Jan A. Grzesik*

Abstract—The celebrated Sommerfeld wedge diffraction solution is reexamined from a null interior field perspective. Exact surface currents provided by that solution, when considered as disembodied half-plane laminae radiating into an ambient, uniform space both inside and outside the wedge proper, do succeed in reconstituting both a specular, mirror field above the exposed face, and a shielding plane-wave field of a sign opposite to that of the incoming excitation which, under superposition, creates both the classical, geometric-optics shadow, and a strictly null interior field at the dominant, plane-wave level. Both mirror and shadow radiated fields are controlled by the residue at just one simple pole encountered during a spectral radiative field assembly, fixed in place by incidence direction ϕ_0 as measured from the exposed face. The radiated fields further provide diffractive contributions drawn from two saddle points that track observation angle ϕ. Even these, more or less asymptotic contributions, are found to cancel exactly within the wedge interior, while, on the outside, they recover in its every detail the canonical structure lying at the base of GTD (geometric theory of diffraction). It is earnestly hoped that this revised scattering viewpoint, while leaving intact all details of the existing solution, will impart to it a fresh, physically robust meaning. Moreover, inasmuch as this viewpoint confirms, admittedly in an extreme limit, the concept of field self-consistency (known in rather more picturesque language as Ewald-Oseen extinction), perhaps such explicit vindication may yet encourage efforts to seek exact solutions to scattering/diffraction by electromagnetically permeable (i.e., dielectric) wedges, efforts that harness integral equations with polarization/ohmic currents distributed throughout wedge volumes as sources radiating into an ambient, uniform reference medium.

1. INTRODUCTION

This paper seeks to add one small nugget of physical interpretation to the celebrated Sommerfeld solution of electromagnetic diffraction by a perfectly conducting wedge. The elegance of Sommerfeld's symmetry/contour integral solution has proved to be an inextinguishable lure to droves upon droves of other researchers who have complemented it with a multitude of successful attacks along still other lines of comparable ingenuity. The material below makes no pretense whatsoever to extending this theoretical repertoire. On the contrary, it accepts *in toto* the outcome of the existing Sommerfeld theory with the object of imparting to it a modicum of physical insight patently deficient in the overabundant wedge diffraction literature. An informal guide, doubtless incomplete, to wedge diffraction theory appears at paper's end.

What we have in mind is to accept the electric surface currents K which the Sommerfeld formalism requires to flow upon both exposed and, generally speaking, shadow faces, and to build up the fields, both near and far, radiated by these currents. The total electromagnetic field existing everywhere is then regarded as having these radiated fields superposed upon the primary, invariably plane wave excitation.

The physical feature which may, regrettably, provoke an initial urge to repudiate,[†] is that all such fields are regarded as being fully able to penetrate into the wedge metallic interior wherein, of course, it is only their sum which is required to vanish identically. More than that, the radiated fields are obliged to produce not only the specularly reflected wave, but to annihilate also the incoming field throughout the traditional shadow region while maintaining therein nonvanishing diffractive contributions. We propose in the sequel to demonstrate all such features with unambiguous, albeit not entirely trivial analysis.

The null interior field viewpoint which we advocate here has its precedent in, and is indeed but an extreme limit of, the traditional Ewald-Oseen extinction phenomenon, wherein a field impinging upon an electrically permeable obstacle stimulates throughout its interior a polarization/ohmic current distribution which then radiates in its turn in such a manner as to replace (read: extinguish) the incoming, ambient-space field with one more suited to propagation within the (not necessarily uniform) dielectric material. When perfectly conducting metallic obstacles, such as our present wedge, enter into play, the Ewald-Oseen apparatus simply defaults to infinitely thin surface current veneers.

One finds in [1] a collection of rather standard electrodynamic problems viewed under the null interior field aspect. That collection begins indeed on a humble, electrostatic note having a point charge placed in proximity to a perfectly conducting half space, a situation instantly resolved through appeal to the construct of a fictitious interior image of equal magnitude and opposite sign. That formal solution, its modest ingenuity and ready success being given their deserved due, provides an access to a real charge distribution across the half space boundary, a distribution on whose basis one calculates a potential reproducing that of the said image on the exterior, and uniformly cancelling the primary field within. So fortified, and with additional plane/cylinder successes in a genuinely electrodynamic setting, a still further problem on loop excitation of a circular waveguide is quick to show that the null interior field viewpoint (in this latter case, being actually extended across the waveguide metallic exterior) can also be harnessed as an active path to problem solution, and not merely in the role, as here, of an *ex post facto* field dissection. In fact, the loop current evolution in time is taken there to be quite general, its details subsumed under a Laplace transform.

The analysis now given had its genesis in just such a burgeoning Ewald-Oseen background, an analysis which, admittedly, represents the second tier of retrenchment from more lofty ambitions. Initial hopes for success in the use of the Ewald-Oseen principle as an active solution basis for the wedge soon foundered, first when deployed against the permeable wedge, and then against its present, metallic limit. Efforts to salvage at least some of this work have thus nucleated into the present, far more modest *post mortem* interpretation. Nevertheless it is our hope that even this, vastly reduced program may still enjoy some minor scientific merit. It had been presented quite some time ago, under an identical title, at the 1999 IEEE Antennas and Propagation/URSI Symposium in Orlando, Florida, but had to await an epoch of sustained leisure to unshackle it from a necessarily *dépêche* format.

2. SOMMERFELD'S SOLUTION SUMMARIZED

Sommerfeld's initial diffractive solution for a half-plane, a degenerate wedge having 2π as its exterior angle, appeared in [2]. In [3], H. M. MacDonald bypassed Sommerfeld's contour integral *cum* symmetry arguments in favor of a development in eigenfunctions *a priori* adapted to the required boundary conditions. He was thus able to cope with wedge diffraction at arbitrary exterior angles short of 2π, and then Sommerfeld yet again in [4] provided a mature overview of his evolved theory. Widely available also is Sommerfeld's half-plane solution in his volume on optics [5]. Unburdened by the German language barrier of [2] and [4], [5] is available in English translation.

The wedge diffraction geometry is given in Figure 1, with exterior angle γ (reckoned from the horizontal face) and a plane wave excitation $E_{z,inc}(r,\phi) = +\exp(-ikr\cos\{\phi - \phi_0\})$ assumed to be incident from above at azimuth ϕ_0. Guided by common intuition, we expect the primary excitation to vanish across shadow region III, to persist intact across region $I \cup II$, and to be accompanied throughout region I by a specularly reflected, mirror companion $E_{z,mirr}(r,\phi) = -\exp(-ikr\cos\{\phi +$

[†] Recoil of this sort is fashioned largely on the basis of mechanical experience, which insists that solid bodies resist penetration. The weight of this experience, routinely reinforced throughout our lives, automatically spills over into electrodynamics, wherein it initially cries out for a similar interdiction. Such anxieties should be lessened by recognizing that, unlike its mechanical counterpart, electrodynamics ignores hardness *per se* and responds only to charge/current sources, idealized herein as being confined to infinitely thin surface sheets.
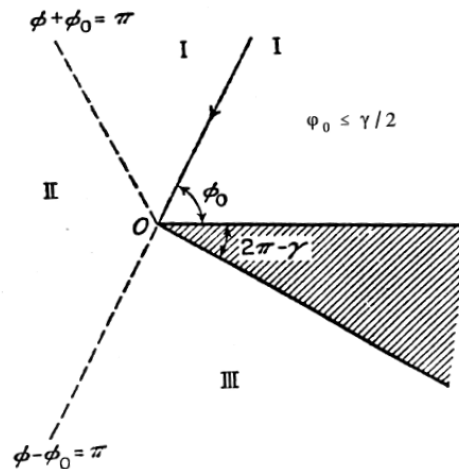
Figure 1. Diffracting wedge geometry.

$\phi_0\}$). Diffractive contributions are expected to creep into all three regions I, II, and III, whereas the perfectly conducting wedge material occupying angular range $\gamma < \phi < 2\pi$ is to be devoid of any electromagnetic penetration. In this simplest of all proof-of-principle problem incarnations, we posit that the incidence direction is to be perpendicular to the edge, which latter naturally serves as the origin $r = 0$ of radial coordinate r complementary to azimuth ϕ, while z, measured positive toward the reader, completes the coordinate triad. Of the two canonical field polarizations, either electric E or magnetic H parallel to the edge, we limit ourselves mostly to the former, with a cursory reference to its partner deferred to Section 11.

As an *ansatz* of great power Sommerfeld introduced the function[‡]

$$v(r, \psi) = \frac{1}{2\gamma} \int\limits_{C_1 \cup C_2} \frac{e^{-ikr\cos\zeta}}{1 - e^{-i\pi(\zeta+\psi)/\gamma}} \, d\zeta \tag{1}$$

vis-à-vis the ζ-plane contours shown in Figure 2. In terms of $v(r, \psi)$ the field pattern $u(r, \phi)$, both near and far, respectively for the E/H polarizations is obtained as

$$u(r, \phi) = v(r, \phi - \phi_0) \mp v(r, \phi + \phi_0). \tag{2}$$

Up to and including Section 10 our concern will be exclusively with the upper, minus sign in Eq. (2), which provides for a null electric field on both wedge faces at $\phi = 0$ and $\phi = \gamma$. It is to be emphasized that Eq. (2) represents the entire field, incident plus that radiated by surface currents K induced on wedge faces.

Figure 1 proclaims the self-evident angular symmetry whereby nothing really new can be encountered by allowing incidence angle ϕ_0 to exceed $\gamma/2$. But even before that, with $\gamma - \pi < \phi_0 < \gamma/2$, it is possible to have both upper and lower wedge faces exposed to the primary illumination, a physically acceptable scenario, to be sure, but one that would complicate the ensuing discussion. Hence, simply on grounds of convenience, we legislate that in fact $0 < \phi_0 < \gamma - \pi$.

Contour $C_1 \cup C_2$ can of course be deformed into $D_1 \cup D_2$ provided that one accounts for the residues at any poles that may crop up within the interval $-\pi < \Re\zeta < \pi$, residues whose form is that of plane waves representing both incoming and all possible specularly reflected contributions. In this way, on the basis of the paragraph preceding, we wish to contend with at most one pole in connection with each of $v(r, \phi \mp \phi_0)$, something now assured by the demand that $0 < \phi_0 < \gamma - \pi$. But, while these precautions do retain an *a priori* validity in the context of contour $C_1 \cup C_2$, they are destined to be shortly superseded by considerations which attach to the alternate contours illustrated in Figures 3–5.

[‡] In standard notation, $k = \omega/c$, with c being the speed of light and ω the angular frequency, taken positive in conformity with integral convergence in the shaded half-strips in Figure 2. Factor $e^{-i\omega t}$, which governs the field temporal variation across the board, is implicitly acknowledged but otherwise hidden from view. All field quantities are dimensionless, normalized by the incoming field amplitude.
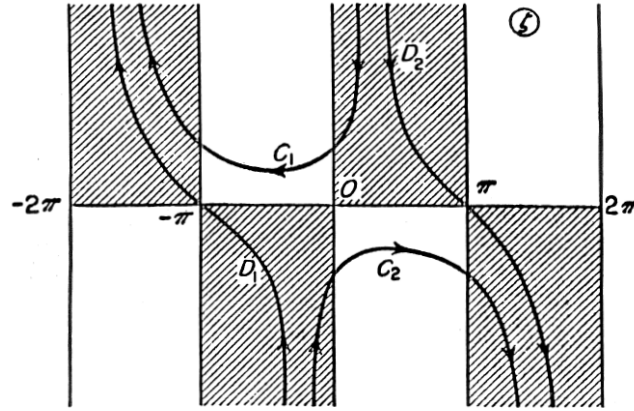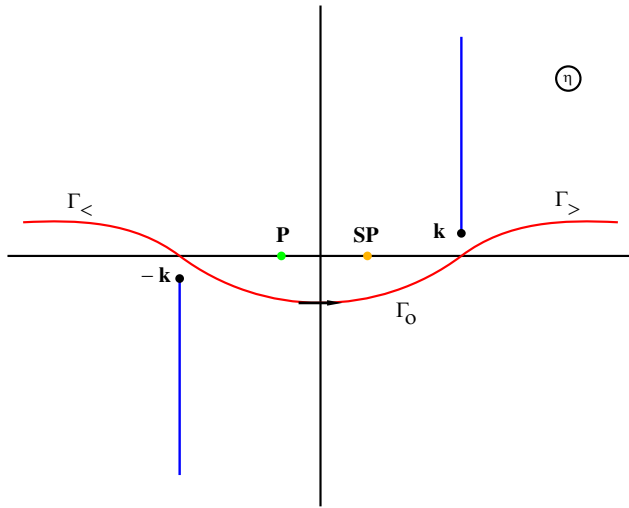
Figure 2. Sommerfeld's canonical contours.

Figure 3. Fourier spectral contour $\Gamma = \Gamma_< \cup \Gamma_0 \cup \Gamma_>$ for Eq. (11).
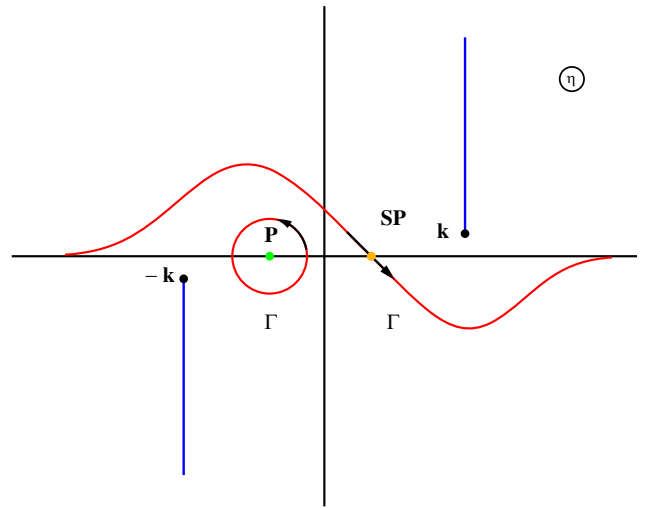
Figure 4. Fourier spectral contour Γ for Eq. (11) within mirror/shielding field regions I and III $\cup$ $\{\gamma < \phi < 2\pi\}$; $\tau = +$.

   Function $u(r, \phi)$ must of course satisfy the Helmholtz equation, a feature automatically underwritten when $v(r, \phi \mp \phi_0)$ individually do so. This latter aspect follows at once by displacing ζ contour $C_1 \cup C_2$ in Eq. (1) through the respective horizontal amounts $\phi \mp \phi_0$, a gesture which exposes to view plane-wave structures $\exp(-ikr \cos\{\zeta - \phi \pm \phi_0\})$ in integrand numerators which, *ipso facto*, validate the Helmholtz constraint. More than this, in order for Eq. (2) to satisfy the E/H boundary conditions, it suffices to require that $v(r, \psi)$ as a function of place holder variable ψ be symmetric around both $\psi = 0$ and $\psi = \gamma$.

   This symmetry attribute is likewise easily verified by noting in Figure 2 that, apart from their sense of traversal, C_1 and C_2 can be freely taken as genuine images of one another under reflection of ζ across
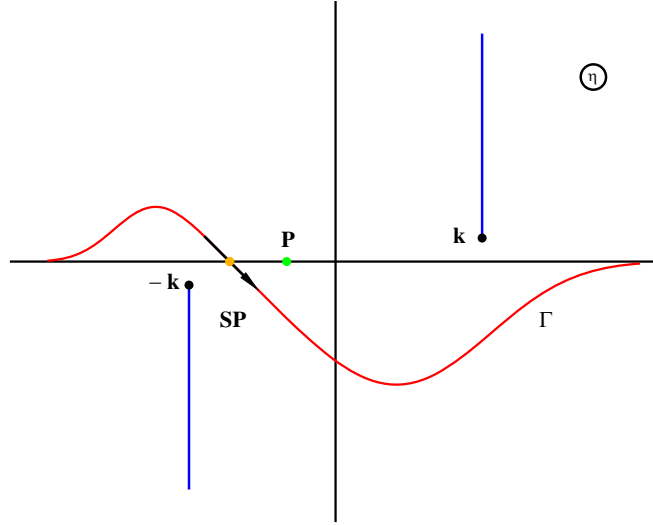
Figure 5. Fourier spectral contour Γ for Eq. (11) in region II illuminated only by diffractive,[§] saddle point contributions; $\tau = +$.

its origin, *viz.*, $\zeta \longleftrightarrow -\zeta$, whence the required place holder symmetries are readily inferred.[‖] But then $v(r, -\phi - \phi_0) = v(r, \phi + \phi_0)$ and $v(r, -\phi + \phi_0) = v(r, \phi - \phi_0)$, and similarly for $\pm\phi$ departures around γ, in consequence of which $u(r, \phi)$ from Eq. (2) with its upper, negative sign on the right is antisymmetric around $\phi = 0$ and $\phi = \gamma$, being thus null and hence adequate to assure a tangential electric boundary condition at both wedge faces. And, for identically the same reasons, a choice of plus sign on the right in Eq. (2) provides a combination symmetric around both $\phi = 0$ and $\phi = \gamma$, whose presumably nonvanishing values there are well adapted to a purely tangential magnetic boundary condition. We observe finally that the confirmed symmetry of $v(r, \psi)$ around both $\psi = 0$ and $\psi = \gamma$ automatically generates, through endless ratcheting that alternates around these two points,[¶] a periodicity in the amount $\psi = 2\gamma$, *viz.*, $v(r, \psi + 2\gamma) = v(r, \psi)$, already evident from the makeup of Eq. (1). It is to Pauli [6] that we owe this seemingly innocent but actually quite crucial observation regarding the symmetry of $v(r, \psi)$ around both $\psi = 0$ and $\psi = \gamma$.

Most of these solution properties are deftly encapsulated in [7], while a more complete discussion can be traced from [8]. In [4] and [8], and to a considerable extent also in [5], one is exposed to a lengthy discourse regarding Riemann surface constructs associated with two-dimensional scattering. In our

---

[§] The qualifier *"illuminated only by diffractive, saddle point contributions"* is to be understood *cum grano salis*, in the sense that the diffractive field contributions due to our wedge surface currents (4)–(5) are of course ultimately destined to be supplemented by the dominant field of the incoming plane wave Eq. (39), as indeed are the mirror/shielding fields to which Figure 4 alludes.

[‖] From Eq. (1) the symmetry around $\psi = \gamma$ emerges as

$$2\gamma v(\gamma - \phi) = \int_{C_1} \frac{e^{-ikr\cos\zeta}}{1 + e^{-i\pi(\zeta-\phi)/\gamma}}\, d\zeta - \int_{C_1} \frac{e^{-ikr\cos\zeta}}{1 + e^{i\pi(\zeta+\phi)/\gamma}}\, d\zeta$$

$$= \int_{C_1} \frac{e^{-ikr\cos\zeta}}{1 + e^{i\pi(\zeta-\phi)/\gamma}} \times e^{i\pi(\zeta-\phi)/\gamma}\, d\zeta - \int_{C_1} \frac{e^{-ikr\cos\zeta}}{1 + e^{-i\pi(\zeta+\phi)/\gamma}} \times e^{-i\pi(\zeta+\phi)/\gamma}\, d\zeta$$

$$= \int_{C_1} \frac{e^{-ikr\cos\zeta}}{1 + e^{-i\pi(\zeta+\phi)/\gamma}}\, d\zeta - \int_{C_1} \frac{e^{-ikr\cos\zeta}}{1 + e^{i\pi(\zeta-\phi)/\gamma}}\, d\zeta = 2\gamma v(\gamma + \phi)\,,$$

and similarly for the symmetry around $\psi = 0$. Passage from the second to the third line above is achieved simply by writing $e^{\pm i\pi(\zeta\mp\phi)/\gamma} = (1 + e^{\pm i\pi(\zeta\mp\phi)/\gamma}) - 1$, with contour C_1 momentarily abridged from above, and then, following an obvious cancellation, allowing that contour to flare out into its vertically unbounded extent.

[¶] A more directly analytic demonstration of the 2γ periodicity emerges on setting

$$v(r, \psi + 2\gamma) = v(r, \gamma + \{\psi + \gamma\}) = v(r, \gamma - \{\psi + \gamma\}) = v(r, -\psi) = v(r, \psi).$$

opinion, the fixed, universal aspect of Figure 2, and a simple recognition of the two symmetries around $\psi = 0$ and $\psi = \gamma$, with a 2γ periodicity noted as an automatic, albeit quite incidental consequence, more than suffice, and that seeking somehow to subordinate it all beneath the mathematical concept of a Riemann surface simply beclouds the intended physical context.

3. SURFACE CURRENT DENSITY ON WEDGE FACES

We set $\tau = \pm$ respectively for the upper ($\phi = 0$) or lower ($\phi = \gamma$) face and, on the strength of the Faraday/Ampère equations combined, find a z-directed current

$$K_z^{(\tau)}(r) = \frac{i\tau}{\omega\mu r}\frac{\partial E_z}{\partial \phi}, \tag{3}$$

wherein the presence of τ as a multiplier acknowledges that the external magnetic field, with just a single, radial component, loops in opposite senses above and below. Symbol μ denotes the uniform magnetic permeability of the ambient space, and sub/superscripts have been permitted to blossom by way of geometric memory prompts. From Eqs. (1) and (2), from the obvious reflection symmetry when $\zeta \longleftrightarrow -\zeta$ between contours C_1 and C_2 as already noted, and with strategic appeal now and then to contour sense reversal, we readily find that

$$K_z^{(\tau)}(r) = \frac{\pi}{\omega\gamma^2\mu r}\left\{ L_z^{(\tau)}(r, \phi_0) - L_z^{(\tau)}(r, -\phi_0) \right\}, \tag{4}$$

with

$$L_z^{(\tau)}(r, \pm\phi_0) = \int_{C_1} e^{-ikr\cos\zeta}\frac{e^{i\pi(\zeta\mp\phi_0)/\gamma}}{(1 - \tau e^{i\pi(\zeta\mp\phi_0)/\gamma})^2}\,d\zeta. \tag{5}$$

4. SURFACE CURRENT DECOMPOSITION INTO A SERIES OF BESSEL FUNCTIONS

On the contour C_1 we are entitled to seek for the integrand in Eq. (5) a convergent power series development, one that opens the door to much useful processing. Easily gotten as the first derivative of a suitable geometric series, this latter reads

$$L_z^{(\tau)}(r, \pm\phi_0) = \tau \sum_{n=1}^{\infty} n\tau^n \int_{C_1} e^{-ikr\cos\zeta}e^{in\pi(\zeta\mp\phi_0)/\gamma}d\zeta, \tag{6}$$

and, because

$$J_p(kr) = -\frac{1}{2\pi}e^{ip\frac{\pi}{2}}\int_{C_1} e^{-i(kr\cos\zeta - p\zeta)}d\zeta, \tag{7}$$

with J_p being a Bessel function whose index p need not be integral [9], it finally condenses into

$$L_z^{(\tau)}(r, \pm\phi_0) = -2\pi\tau \sum_{n=1}^{\infty} n\tau^n e^{-i\frac{n\pi}{\gamma}\left(\frac{\pi}{2}\pm\phi_0\right)} J_{\frac{n\pi}{\gamma}}(kr). \tag{8}$$

One may remark in passing that, in seeking a series development at this point, we are in a sense unraveling, but only momentarily so, the path to solution adopted in [3].

5. SHEET RADIATION DETERMINED BY THE FOURIER TRANSFORM OF ITS CURRENT SOURCE

Once currents $K_z^{(\tau)}(r)$, $\tau = \pm$, are duly in hand,[+] we proceed with field computation on the premise that henceforth they radiate, both up and down, within the ambient medium characterized by magnetic

---

[+] We stress yet again that these currents have arisen in response to the *total* field, incident superposed upon that self-consistently radiated in the context of the *bona fide*, metallic wedge.

permeability μ as already introduced, dielectric permittivity ϵ, and a vanishing conductivity $\sigma \downarrow 0+$, all three parameters being deemed to be uniform in both space and time. We introduce moreover generic Cartesian coordinates $\{\hat{x}, \hat{y}\}$, tailored as necessary to the two laminae:

$$\begin{pmatrix} \hat{x} \\ \hat{y} \end{pmatrix} = \begin{pmatrix} r\cos\phi \\ r\sin\phi \end{pmatrix} \tag{9}$$

when $\tau = +$, and

$$\begin{pmatrix} \hat{x} \\ \hat{y} \end{pmatrix} = \begin{pmatrix} r\cos(\phi - \gamma) \\ r\sin(\phi - \gamma) \end{pmatrix} \tag{10}$$

when instead $\tau = -$. With this notation, which tethers all geometry to the master $\{r, \phi\}$ polar coordinates implied in Figure 1, we can resolve both radiated fields in terms of their respective spectra $A^{(\tau)}(\eta)$ of generalized plane waves

$$E_z^{(\tau)}(\hat{x}, \hat{y}) = \int_{-\infty}^{\infty} e^{i\eta\hat{x} - |\hat{y}|\sqrt{\eta^2 - k^2}} A^{(\tau)}(\eta)\, d\eta \tag{11}$$

in both their propagating (when $\eta^2 < k^2$) and evanescent (when $\eta^2 > k^2$) incarnations. Strictly speaking

$$k = \lim_{\sigma \downarrow 0+} \omega \sqrt{\epsilon\mu\{1 + i\sigma/(\omega\epsilon)\}} \tag{12}$$

has a vanishing imaginary part so that the sharpness of the propagating/evanescent transition makes sense only when understood, by common convention, as an attribute only of that real limit. Furthermore, when, as here, angular frequency ω is taken as positive, branch cuts for the square root may be taken up and down respectively from $\pm k$, optimally approaching the imaginary axis.[⋆]

Now, since currents $K_z^{(\tau)}(r)$, $\tau = \pm$, are here viewed as disembodied entities floating in the ambient space, we can harness the Faraday-Ampère duo along either sheet with $\hat{y} = 0$ in the form

$$\frac{2}{i\omega\mu} \int_{-\infty}^{\infty} e^{i\eta\hat{x}} \sqrt{\eta^2 - k^2} A^{(\tau)}(\eta)\, d\eta = \begin{cases} 0; & \hat{x} < 0 \\ K_z^{(\tau)}(\hat{x}); & \hat{x} > 0 \end{cases} \tag{13}$$

requiring no further qualification as to magnetic field direction and yielding

$$A^{(\tau)}(\eta) = \frac{i\omega\mu}{4\pi\sqrt{\eta^2 - k^2}} \int_0^{\infty} e^{-i\eta r} K_z^{(\tau)}(r)\, dr \tag{14}$$

under inverse Fourier transformation. The incoming field, being continuous, is powerless to make any contribution to Eq. (13) on its left.

6. INVOKING THE WEBER-SCHAFHEITLIN INTEGRAL

Reference to Eqs. (4) and (8) shows that Eq. (14) obliges us to consider next the Weber-Schafheitlin integral

$$M_n = \int_0^{\infty} e^{-i\eta r} r^{-1} J_{\frac{n\pi}{\gamma}}(kr)\, dr. \tag{15}$$

An adaptation of the work in [11] then readily gives, with η temporarily regarded as purely real,

$$M_n = \left(\frac{\gamma}{n\pi}\right) k^{-\frac{n\pi}{\gamma}} \times \begin{cases} e^{-i\frac{n\pi^2}{2\gamma}} \left\{ \eta - \sqrt{\eta^2 - k^2} \right\}^{\frac{n\pi}{\gamma}} \\ e^{-i\frac{n\eta\pi^2}{2|\eta|\gamma}} \left\{ |\eta| - \sqrt{\eta^2 - k^2} \right\}^{\frac{n\pi}{\gamma}} \end{cases} \tag{16}$$

[⋆] The preferred branch cuts join Riemann sheets on which $\Re\sqrt{\eta^2 - k^2}$ is uniformly of opposite sign. The cuts themselves are thus defined by $\Re\sqrt{\eta^2 - k^2} = 0$. This has the pleasant consequence that contours may be dilated into upper/lower semicircular arcs at infinity which, of themselves, beget no contributions, the end results, save for residues, if any, being the surviving loops around said branch cuts. All of this, however, is without bearing upon our further arguments, as a result of which we have simplified our Figures 3–5 by portraying branch cuts that point straight up or down. The *raison d'être* for such preferred, curved branch cut geometry is more full explicated in [10], 20–23.

respectively for $|\eta| \leq k$ and $|\eta| > k$.

Anticipating next the summation stipulated by Eq. (8), we see that the overt index multiplier n conveniently disappears, and that convergence is quite unhindered for $|\eta| > k$. This latter assertion follows by setting $|\eta| = k \cosh \theta$, real $\theta > 0$, whence also

$$|\eta| - \sqrt{\eta^2 - k^2} = k \left\{ \cosh \theta - \sinh \theta \right\} = k e^{-\theta}. \tag{17}$$

For $|\eta| \leq k$, by contrast, since a similar parametrization as $\eta = k \cos \vartheta$ over $0 \leq \vartheta \leq \pi$ yields

$$\eta - \sqrt{\eta^2 - k^2} = k e^{i\vartheta}, \tag{18}$$

it follows that convergence is assured by permitting ϑ to migrate *upward* in its own complex plane, $\vartheta = \alpha + i\beta$, $0 \leq \alpha \leq \pi$, $\beta > 0$, an excursion which, with a view to

$$\eta = k \cos(\alpha + i\beta) = k \left\{ \cos \alpha \cosh \beta - i \sin \alpha \sinh \beta \right\}, \tag{19}$$

has the effect of depressing the Fourier spectral contour Γ for Eq. (11) *downward* when $-k < \Re \eta < k$.[†] The resulting contour, complete with its downward bulge, appears in Figure 3 as a composite of three contiguous pieces, $\Gamma = \Gamma_< \cup \Gamma_0 \cup \Gamma_>$. Figure 3 serves in addition to presage the existence of a simple pole (**P**, colored green and situated to the left of the imaginary axis as befits the arbitrary choice $\phi_0 < \pi/2$ depicted in Figure 1; *cf.* first line after Eq. (25) below) and a saddle point (**SP**, colored sandy beige), both lying on the real η axis. In particular, their relative order will shortly be seen to dictate two distinct categories of preferred deformations for Γ, deformations which convey a most natural distinction between diffracted, and the dominant, reflected/shielding fields.

Of course, once convergent summations have been duly attained under the careful gaze of Eqs. (18)–(19), we are given a *carte blanche* to exploit the benefits of contour deformation as far as analyticity may allow.

7. SERIES SUMMATION IN REVERSE

Now that the radial quadrature mandated in Eq. (14) has been disposed of, our next step in the buildup of spectral amplitudes $A^{(\tau)}(\eta)$ is to perform the sums

$$N_\pm^{(\tau)}(\eta) = -2\pi\tau \left(\frac{\pi}{\omega \gamma^2 \mu} \right) \sum_{n=1}^{\infty} n \tau^n e^{-i\frac{n\pi}{\gamma} \left(\frac{\pi}{2} \pm \phi_0 \right)} M_n \tag{20}$$

on which the interplay of Eqs. (4) and (8) insists. A glance at Eq. (16) reveals that these are again in the nature of geometric series, and give

$$N_\pm^{(\tau)}(\eta) = - \left(\frac{2\pi}{\omega \gamma \mu} \right) e^{-i\frac{\pi}{\gamma}(\pi \pm \phi_0)} k^{-\frac{\pi}{\gamma}} \times \begin{cases} \dfrac{\left\{ \eta - \sqrt{\eta^2 - k^2} \right\}^{\frac{\pi}{\gamma}}}{1 - \tau e^{-i\frac{\pi}{\gamma}(\pi \pm \phi_0)} k^{-\frac{\pi}{\gamma}} \left\{ \eta - \sqrt{\eta^2 - k^2} \right\}^{\frac{\pi}{\gamma}}} \\[4ex] \dfrac{e^{i\frac{\pi^2}{2\gamma}(1-\eta/|\eta|)} \left\{ |\eta| - \sqrt{\eta^2 - k^2} \right\}^{\frac{\pi}{\gamma}}}{1 - \tau e^{-i\frac{\pi}{\gamma}(\pi \pm \phi_0)} e^{i\frac{\pi^2}{2\gamma}(1-\eta/|\eta|)} k^{-\frac{\pi}{\gamma}} \left\{ |\eta| - \sqrt{\eta^2 - k^2} \right\}^{\frac{\pi}{\gamma}}} \end{cases} \tag{21}$$

respectively for $|\eta| \leq k$ and $|\eta| > k$.

8. FIELD RECOVERY: POLE AND SADDLE POINTS

On collating Eqs. (4), (8), (11), (14)–(16), and (20)–(21), in that order, we are led to consider the auxiliary quantities

$$O_\pm^{(\tau)}(\hat{x}, \hat{y}) = \frac{i\omega\mu}{4\pi} \int_\Gamma e^{i\eta\hat{x} - |\hat{y}|\sqrt{\eta^2 - k^2}} \frac{N_\pm^{(\tau)}(\eta)}{\sqrt{\eta^2 - k^2}} d\eta \tag{22}$$

[†] A *downward* contour shift of this sort is compatible with the analyticity prospects already suggested by Eq. (14).

whose difference

$$E_z^{(\tau)}(\hat{x}, \hat{y}) = O_+^{(\tau)}(\hat{x}, \hat{y}) - O_-^{(\tau)}(\hat{x}, \hat{y}) \tag{23}$$

provides at length the field radiated by the upper/lower wedge face respectively as $\tau = \pm$.

We shall not attempt any evaluation of Eq. (23) for observation points $\{\hat{x}, \hat{y}\}$ close to the diffractive edge. Nowadays such evaluation can, if all else fails, be reasonably undertaken through outright numerical quadrature. Physical insight greater by far is bestowed on Eq. (23) by passing at once to sufficiently remote field points and recognizing that Eqs. (21) and (22) taken together usher in a simple pole, fixed in place by incidence angle ϕ_0, and a pair of saddle points which respond to movement on the part of observation angle ϕ. An approach to, and ultimate transit across that simple pole, on the part of one such saddle point, undertaken from both directions, has a vivid interpretation as a shadow boundary crossing. Such transit occurs at both *bona fide* shadow (II–III: $\phi_{geom\,opt} = \pi + \phi_0$) and specular reflection (I–II: $\phi_{mirror} = \pi - \phi_0$) boundaries.

Our computational strategy unfolds henceforth by deforming spectral contour Γ so as to traverse each saddle point individually, their locations shortly to be characterized, along proper, steepest descent paths at a more or less standard, $\pi/4$ declination. A pole may or may not be crossed during this redeployment and, if it is, account is made of its residue. This latter, residue part of the calculation is not inherently asymptotic and, indeed, it will be seen that the two separate pole crossings individually switch, first off, and then on, the traditional reflected and the now eagerly sought shadowing fields, in that order, as ϕ sweeps out its full range from 0 to 2π.

8.1. Simple Pole Fixed Location

In Eq. (17) we have shown, when $|\eta| > k$ and with some real positive θ, that

$$\left\{ |\eta| - \sqrt{\eta^2 - k^2} \right\} / k = e^{-\theta} < 1, \tag{24}$$

which clearly denies $N_\pm^{(\tau)}(\eta)$ any possibility of exhibiting real axis poles outside the canonical interval $-k < \eta < k$. For such real axis poles one must accordingly turn to the first line in Eq. (21), which latter posits that, if they occur at all, they must do so when

$$1 - \tau e^{-i\frac{\pi}{\gamma}(\pi \pm \phi_0)} k^{-\frac{\pi}{\gamma}} \left\{ \eta - \sqrt{\eta^2 - k^2} \right\}^{\frac{\pi}{\gamma}} = 1 - \tau e^{-i\frac{\pi}{\gamma}\left\{ \pi \pm \phi_0 - \alpha_{p,\pm}^{(\tau)} \right\}} = 0 \,. \tag{25}$$

For $\tau = +$, the upper wedge face being designated as source, we clearly have $\alpha_{p,-}^{(+)} = \pi - \phi_0$ as the single possible candidate.[♯] For $\tau = -$, by contrast, when it is the lower face which radiates, we require that

$$(\pi/\gamma) \times \left(\pi \pm \phi_0 - \alpha_{p,\pm}^{(-)} \right) = \pi \tag{26}$$

whence

$$\alpha_{p,\pm}^{(-)} = \pi \pm \phi_0 - \gamma < 0, \tag{27}$$

both of which reside exterior to our preferred interval[‡‡] and thus cannot beget residues.

We shall defer disclosing the residue results at simple pole $k \cos\{\alpha_{p,-}^{(+)}\} = k \cos(\pi \pm \phi_0) = -k \cos\phi_0$ until the accompanying saddle point movement has been brought into sharper focus.

8.2. Saddle Point Moveable Locations

Unlike the pole at $k \cos\{\alpha_{p,-}^{(+)}\}$, which is fixed once incidence direction ϕ_0 has been specified, the saddle points $k \cos\{\alpha_{sp}^{(\tau)}\}$, while remaining indifferent to the exterior $\pm$ partition called for in Eq. (23), do respond to both observation angle ϕ and wedge face marker τ. The saddle point field contributions themselves respond to all available parameters.

[♯] The other candidate verifying $\pi + \phi_0 - \alpha_{p,+}^{(+)} = 0$ or else $\alpha_{p,+}^{(+)} = \pi + \phi_0 > \pi$ is disqualified by falling beyond the permissible interval.
[‡‡] One arrives at an identical conclusion if π on the right in Eq. (26) is replaced by $m\pi$ for any odd integer m, positive or negative at will.

When observation radius r is sufficiently large, and together with it $\hat{x}$ and/or $\hat{y}$ are similarly so in magnitude, one can resort to a saddle point approximation to the four quantities $O_\pm^{(\tau)}(\hat{x}, \hat{y})$ subsumed beneath Eq. (22). The two saddle points which now emerge are routinely found by requiring that the derivative of the phase in Eq. (22) vanish. Thus

$$\frac{d\left\{i\eta\hat{x} - |\hat{y}|\sqrt{\eta^2 - k^2}\right\}}{d\eta} = 0 \tag{28}$$

whence it follows that

$$\hat{x} = \frac{\eta|\hat{y}|}{\sqrt{k^2 - \eta^2}}. \tag{29}$$

Reference to Eqs. (9) and (10) then shows that Eq. (29) amounts to

$$\cos\alpha|\sin\phi| = \sin\alpha\cos\phi \tag{30}$$

when $\tau = +$, and

$$\cos\alpha|\sin(\phi - \gamma)| = \sin\alpha\cos(\phi - \gamma) \tag{31}$$

if instead $\tau = -$. And so it becomes a consistent gesture to set

$$\alpha_{sp}^{(+)} = \begin{cases} \phi; & 0 < \phi < \pi \\ 2\pi - \phi; & \pi < \phi < 2\pi, \end{cases} \tag{32}$$

and

$$\alpha_{sp}^{(-)} = \begin{cases} \phi - \gamma; & 0 < \phi - \gamma < \pi \\ 2\pi - \phi + \gamma; & \pi < \phi - \gamma < 2\pi \end{cases} \tag{33}$$

by way of assuring that $0 < \alpha_{sp}^{(\pm)} < \pi$ and hence that $\sin\alpha_{sp}^{(\pm)} > 0$. Assured in fact are the more precise equalities $\sin\alpha_{sp}^{(+)} = |\sin\phi|$ and $\sin\alpha_{sp}^{(-)} = |\sin(\phi - \gamma)|$.

We note that both saddle point locations $k\cos\{\alpha_{sp}^{(\pm)}\}$ traverse the canonical slot $(-k, k)$ twice, first backward and then forward, during the course of a full, $0 < \phi < 2\pi$ angular ambit. During such full circumnavigation, saddle point $k\cos\{\alpha_{sp}^{(+)}\}$ must contend with an encroachment, both fore and aft, upon simple pole $k\cos\{\alpha_{p,-}^{(+)}\}$, whereas $k\cos\{\alpha_{sp}^{(-)}\}$ is exempt from any similar complication, there being now no corresponding poles $k\cos\{\alpha_{p,\pm}^{(-)}\}$ in play. This distinction finds a graphic embodiment in the fact that steepest descent passage through $k\cos\{\alpha_{sp}^{(+)}\}$ requires contour Γ deformation of both categories depicted in Figures 4 and 5, whereas passage through $k\cos\{\alpha_{sp}^{(-)}\}$ follows Figure 5 only *ad libitum*, but of course with no pole (green dot) present. For imminent use in Eqs. (41)–(44), and at considerable risk of belaboring the point, we emphasize that Eqs. (32) and (33) can also be restated as

$$\begin{cases} \cos\alpha_{sp}^{(+)} = \cos\phi; & 0 < \phi < 2\pi \\ \sin\alpha_{sp}^{(+)} = |\sin\phi|; & 0 < \phi < 2\pi \end{cases} \tag{34}$$

and

$$\begin{cases} \cos\alpha_{sp}^{(-)} = \cos(\phi - \gamma); & 0 < \phi < 2\pi \\ \sin\alpha_{sp}^{(-)} = |\sin(\phi - \gamma)|; & 0 < \phi < 2\pi . \end{cases} \tag{35}$$

8.3. Saddle Point Pole Crossings

We can now summarize as follows the cooperative pole/saddle point evaluations as we traverse the full angular range, $0 < \phi < 2\pi$, including in our mind's eye the wedge interior. As we move outward from $\phi = 0$ in region I, the saddle point $\eta_{sp}^{(+)} = k\cos\{\alpha_{sp}^{(+)}\}$ slides steadily downward from $\eta_{sp}^{(+)} = k$. Saddle point crossing on behalf of $-O_-^{(+)}(r\cos\phi, r\sin\phi)$ in region I can evidently occur only if inversion contour Γ from Figure 3 had first been subjected to a deformation as conveyed in Figure 4, engendering

an isolated loop around the pole at $\eta_{p,-}^{(+)} = k\cos\{\alpha_{p,-}^{(+)}\}$. The residue contribution from that pole is thus present throughout region I, wherein it conveys the specular, mirror companion of the incident plane wave, the latter only implicitly present in our radiative field buildup. The coexisting saddle point contribution is to be regarded hence as a diffractive, even if only an approximate correction.

As is universally recognized, the validity of this diffractive correction clearly deteriorates on saddle point approach to the pole, but, following observation point transit from region I into region II (regions II and III, and the wedge interior $\gamma < \phi < 2\pi$ being deemed in shadow *vis-à-vis* the mirror field), regains its assigned level of validity.[§§]

Once ϕ enters region II, the mirror/residue field is abruptly switched off, only to resume as a shielding field on entry into region III. As in the $I \to II$ transition, localized caveats as to saddle point accuracy briefly flare into view around the moment of shielding/residue field ignition. Indeed, the shielding field remains lit throughout region III *and* the wedge interior combined, $\pi + \phi_0 < \phi < 2\pi$. And then, once the incident field is at long last brought into play, it illuminates regions I and II but, across $\pi + \phi_0 < \phi < 2\pi$ (region III plus wedge interior) it is extinguished by the shielding field.

Additional diffractive, saddle point radiative field contributions flow also from $O_+^{(+)}(r\cos\phi, r\sin\phi)$, and $\pm O_\pm^{(-)}(r\cos\{\phi - \gamma\}, r\sin\{\phi - \gamma\})$ across the full angular range, unburdened by any concern about pole encounters. But of course the cumulative effect of them all, including that of $-O_-^{(+)}(r\cos\phi, r\sin\phi)$ under present view, does vanish exactly within wedge interior $\gamma < \phi < 2\pi$, as one easily verifies when equipped with the saddle point evaluations soon to follow. Such diffractive cancellation on wedge interior is itself a most welcome manifestation of radiative shielding.

The distinction between the required deformations of spectral contour Γ, before and after the first shadow crossing, $I \to II$, is illustrated in Figures 4 and 5. Contour structure 5 clearly reverts to that of 4 on the subsequent entry $II \to III$ into the classical shadow. It bears repeating, perhaps, that these two deformation categories pertain only to the steepest descent path through $k\cos\{\alpha_{sp}^{(+)}\}$, while for partner $k\cos\{\alpha_{sp}^{(-)}\}$ Figure 5 will suffice, with its green dot suppressed.

9. SHIELDING AND MIRROR FIELD CONTRIBUTIONS

And so, as we cross from region II into either region I or else region III *cum* wedge, the pole contribution $E_{z,p}(r, \phi)$ lights up and, so to speak, remains lit. Residue evaluation at $\eta_{p,-}^+ = k\cos\{\alpha_{p,-}^{(+)}\} = k\cos(\pi - \phi_0) = -k\cos\phi_0$ as guided by the first line from Eq. (21) yields, after an elementary albeit mildly tedious computation,

$$E_{z,p}(r, \phi) = -e^{-ikr(\cos\phi_0\cos\phi - \sin\phi_0|\sin\phi|)}, \tag{36}$$

which is nothing other than the specular, mirror field

$$E_{z,mirr}(r, \phi) = -e^{-ikr(\cos\phi_0\cos\phi - \sin\phi_0\sin\phi)} = -e^{-ikr\cos(\phi + \phi_0)} \tag{37}$$

when $0 < \phi < \pi - \phi_0$, and

$$E_{z,shield}(r, \phi) = -e^{-ikr(\cos\phi_0\cos\phi + \sin\phi_0\sin\phi)} = -e^{-ikr\cos(\phi - \phi_0)} \tag{38}$$

when instead $\pi + \phi_0 < \phi < 2\pi$. A final, blanket superposition everywhere of the incident field

$$E_{z,inc}(r, \phi) = +e^{-ikr\cos(\phi - \phi_0)} \tag{39}$$

illuminates regions I and II, and is fully extinguished by $E_{z,shield}(r, \phi)$ from Eq. (38) across region III, the traditional geometric optics shadow, and throughout the wedge interior, $\gamma < \phi < 2\pi$. Our mirror/shielding claims have thus been vindicated, at least at the dominant, plane wave level.

It is somehow pleasing to one's physical sensibilities that both dominant fields, mirror and shielding, can be ascribed to just $-O_-^{(+)}(r\cos\phi, r\sin\phi)$, whose radiative source resides in that portion of the

---

[§§] People have devised various stratagems to mitigate saddle point failure in pole proximity. One such can found in [12] and [13]. On the other hand, there is clearly no *a priori* physical reason for the apparent saddle point failure, one that entails a spurious divergence, and is simply an unintended artifact of pretending that a pole may be permitted to sit astride a steepest descent contour. In fact, inversion contour Γ from Figure 3 need not submit to the additional distortions in Figures 4 and 5, and does so only in the hope of procuring thereby some numerically useful and physically satisfying approximations.

currents which flow across the upper, exposed wedge face. That portion, moreover, is associated with the term $-v(r, \phi + \phi_0)$, present in Eq. (2) so as to maintain the angular symmetries that underlie the electric boundary condition now in force. By contrast, saddle point contributions from all four terms, $O_{\pm}^{(\pm)}(\hat{x}, \hat{y})$, each suitably evaluated in Eq. (43) below, must be pressed into cooperative service so as to resurrect the canonical GTD diffractive field in Eq. (47) on wedge exterior and, remarkably, but also unavoidably, so as to vanish exactly, Eq. (46), across its interior, $\gamma < \phi < 2\pi$.

10. DIFFRACTIVE FIELD CONTRIBUTIONS

An *apropos* moment has arrived to add in the diffractive, saddle point contributions $O_{\pm}^{(\tau,sp)}(\hat{x}, \hat{y})$ and to demonstrate that their sum

$$E_z^{(sp)}(r, \phi) = \sum_{\tau=\pm} \sum_{\zeta=\pm} \zeta\, O_{z,\zeta}^{(\tau,sp)}(\hat{x}, \hat{y}) \tag{40}$$

properly vanishes within wedge interior $\gamma < \phi < 2\pi$, whereas across the entire wedge exterior $0 < \phi < \gamma$, save for narrow angular exclusion slivers around shadow boundaries $\phi_{\pm,shad} = \pi \pm \phi_0$, as previously described, it reproduces the standard foundation for the geometric theory of diffraction.

Adhering thus to a well worn recipe, we are instructed to approximate the phase $\Phi^{(\tau)}$ in Eq. (22) through the second order in the departure of η from $\eta_{sp}^{(\tau)} = k \cos\{\alpha_{sp}^{(\tau)}\}$. For a phase $\Phi^{(\tau)}$ so curtailed we find

$$\Phi^{(\tau)} \approx ik\hat{x} \cos\left\{\alpha_{sp}^{(\tau)}\right\} + ik|\hat{y}| \sin\left\{\alpha_{sp}^{(\tau)}\right\} - \frac{i|\hat{y}|}{2k\sin^3\left\{\alpha_{sp}^{(\tau)}\right\}} \left(\eta - k\cos\left\{\alpha_{sp}^{(\tau)}\right\}\right)^2, \tag{41}$$

which reveals a steepest descent direction aligned along $e^{-i\pi/4}$ and, by virtue of Eqs. (9)–(10) and (34)–(35) combined, simplifies to just

$$\Phi^{(\tau)} \approx ikr - \frac{i|\hat{y}|}{2k\sin^3\left\{\alpha_{sp}^{(\tau)}\right\}} \left(\eta - k\cos\left\{\alpha_{sp}^{(\tau)}\right\}\right)^2. \tag{42}$$

The Gaussian integral which now confronts us is performed in routine fashion, the upshot of it all being that

$$O_{z,\pm}^{(\tau,sp)}(\hat{x}, \hat{y}) = \frac{1}{\gamma}\sqrt{\frac{\pi}{2kr}}\, e^{i(kr-\pi/4)} \frac{e^{-i\pi(\pi\pm\phi_0)/\gamma}\Lambda_\tau^{\pi/\gamma}}{1 - \tau e^{-i\pi(\pi\pm\phi_0)/\gamma}\Lambda_\tau^{\pi/\gamma}} \tag{43}$$

with

$$\Lambda_\tau = \begin{cases} \cos\phi + i|\sin\phi|; & \tau = + \\ \cos(\phi-\gamma) + i|\sin(\phi-\gamma)|; & \tau = - \end{cases} \tag{44}$$

itself discriminating between upper and lower wedge faces.

The structure of Eq. (44) further forces us to distinguish between regions above and below with respect to each individual lamina. A complete, $0 < \phi < 2\pi$ circuit around the origin is thus partitioned in accordance with

$$\begin{cases} 0 < \phi < \gamma - \pi: & \Lambda_+ = e^{i\phi}, & \Lambda_- = e^{i(\phi-\gamma+2\pi)} \\ \gamma - \pi < \phi < \pi: & \Lambda_+ = e^{i\phi}, & \Lambda_- = e^{i(\gamma-\phi)} \\ \pi < \phi < \gamma: & \Lambda_+ = e^{i(2\pi-\phi)}, & \Lambda_- = e^{i(\gamma-\phi)} \\ \gamma < \phi < 2\pi: & \Lambda_+ = e^{i(2\pi-\phi)}, & \Lambda_- = e^{i(\phi-\gamma)}. \end{cases} \tag{45}$$

Parametrization in Eq. (18) requires moreover that all instances of $\Lambda_\tau = \exp(i\vartheta_\tau)$ have their angular arguments constrained by $0 < \vartheta_\tau < \pi$. The 2π phase shift in the first, third, and fourth lines stands in testimony to such adjustments, as do the angular reversals in the second through fourth. It is implicitly assumed (see Fig. 1) that $\pi < \gamma < 2\pi$, so as to bypass face-to-face mirror bounce complications and to retain an option to sidestep mirror reflection from both wedge faces. Simple, albeit mildly tedious calculations based on Eqs. (40), (43), and (45) inform us finally that

$$E_z^{(sp)}(r, \phi) = \sum_{\tau=\pm} \sum_{\zeta=\pm} \zeta\, O_{z,\zeta}^{(\tau,sp)}(\hat{x}, \hat{y}) = 0, \tag{46}$$

a *bona fide* diffractive cancellation throughout the wedge interior, $\gamma < \phi < 2\pi$, whereas on its exterior, $0 < \phi < \gamma$, save for the exclusion slivers at shadow boundaries as previously mentioned, we find

$$E_z^{(sp)}(r,\phi) = \sum_{\tau=\pm} \sum_{\zeta=\pm} \zeta \, O_{z,\zeta}^{(\tau,sp)}(\hat{x},\hat{y})$$

$$= \frac{1}{\gamma}\sqrt{\frac{\pi}{2kr}}\, e^{i(kr+\pi/4)} \left[\frac{\sin(\pi^2/\gamma)}{\cos\left(\frac{\pi^2}{\gamma}\right) - \cos\left(\frac{\pi\{\phi-\phi_0\}}{\gamma}\right)} - \frac{\sin(\pi^2/\gamma)}{\cos\left(\frac{\pi^2}{\gamma}\right) - \cos\left(\frac{\pi\{\phi+\phi_0\}}{\gamma}\right)} \right], \quad (47)$$

the very cradle indeed of GTD, with boundary conditions properly obeyed at both $\phi = 0$ and $\phi = \gamma$.

11. MAGNETIC FIELD PARALLEL TO EDGE

When the incident, and therefore the entire magnetic field **H** is purely edge directed, with but a single component H_z (the so-called TM case, $+$ sign in Eq. (2)), electric surface current **K** shifts orientation from being purely axial to purely outgoing, perpendicular to the edge. In the natural coordinate system of either radiating face we confront now the surface current component $K_{\hat{x}} = K_r$ and, as the analogue to spectral representation in Eq. (11) we get

$$H_z^{(\tau)}(\hat{x},\hat{y}) = \text{sign}(\hat{y}) \int_{-\infty}^{\infty} e^{i\eta\hat{x}-|\hat{y}|\sqrt{\eta^2-k^2}} C^{(\tau)}(\eta)\, d\eta, \quad (48)$$

with spectral amplitude $C^{(\tau)}(\eta)$ replacing the previous $A^{(\tau)}(\eta)$. A simple use of Ampère's law, followed by the obligatory Fourier inversion, permits one yet again to render spectral amplitude $C^{(\tau)}(\eta)$ in terms of current density $K_r^{(\tau)}(r)$, *viz.,*

$$C^{(\tau)}(\eta) = \frac{1}{4\pi} \int_0^{\infty} e^{-i\eta r} K_r^{(\tau)}(r)\, dr. \quad (49)$$

Past this point the remainder of the program unfolds pretty much as before. We recover the dominant shielding and mirror field contributions *à la* Section 9, phrased now in terms of $H_z(r,\phi)$, the mirror field confined to Region I and the shielding extended across the augmented $III \cup \{\text{wedge interior}\}$ angular domain $\pi + \phi_0 < \pi < 2\pi$. The saddle-point diffractive counterpart to Eq. (47)

$$H_z^{(sp)}(r,\phi) = \frac{1}{\gamma}\sqrt{\frac{\pi}{2kr}}\, e^{i(kr+\pi/4)} \left[\frac{\sin(\pi^2/\gamma)}{\cos\left(\frac{\pi^2}{\gamma}\right) - \cos\left(\frac{\pi\{\phi-\phi_0\}}{\gamma}\right)} + \frac{\sin(\pi^2/\gamma)}{\cos\left(\frac{\pi^2}{\gamma}\right) - \cos\left(\frac{\pi\{\phi+\phi_0\}}{\gamma}\right)} \right], \quad (50)$$

on wedge exterior $0 < \phi < \gamma$ is gotten under a simple sign reversal from minus to plus on the right, and coexists with a rigorously null magnetic field (at this level of approximation) on wedge interior $\gamma < \phi < 2\pi$.

12. PARTING COMMENTS

Were we to relax the angular constraint, so that $\gamma/2 > \phi_0 > \gamma - \pi$, then, in contrast to Eq. (27), there would appear a fresh simple pole with $\alpha_{p,+}^{(-)} = \pi + \phi_0 - \gamma > 0$ accompanied, on the physical side, by additional mirror/shielding fields. Such a scenario would require a similar, albeit more robust treatment on its own terms, something that we have avoided in the interest of methodological simplicity.

Furthermore, as we have previously mentioned, the present work, already at some modest level of intricacy, is but a retrenchment, a reluctant retreat from the far more ambitious goal to which we had initially aspired, which is to say, to actually base a wedge diffraction apparatus entirely upon an *a priori* null interior field demand. So magisterial a goal has so far proved to lie well beyond our reach. And, if one is thus forced to admit defeat when faced by a perfectly conducting obstacle, how much dimmer must be any solution prospects when contemplating the permeable, dielectric wedge, one which no longer enjoys, even implicitly, anything akin to the crucial symmetries $v(-\phi) = v(\phi)$ and

$v(\gamma - \phi) = v(\gamma + \phi)$? Such perceived difficulties notwithstanding, we continue to entertain the hope that exact solutions to scattering/diffraction by electromagnetically permeable, dielectric wedges may yet be attained on the basis of field self-consistency, couched in the framework of integral equations which superpose the self-consistent radiation from current sources distributed across wedge interiors.

13. A BIBLIOGRAPHIC POTPOURRI

We wish to assemble here an informal, occasionally opinionated, *ad hoc* miniguide to the voluminous literature devoted to wedge diffraction and to its specialized half-plane subset gotten when $\gamma = 2\pi$. Contemporary work, with much emphasis on wedge surface currents, is exemplified by [14]. Somewhat more recent is the review [15], valuable for both its richly illustrated content and an ample bibliography. One of its three authors is Pyotr Yakovlevich Ufimtsev, the acknowledged father of the physical theory of diffraction, wherein physical emphasis is displaced, as here, from field boundary conditions as a prime focus of concern, to the actual surface currents that are the true sources of radiation [16]. At some remove in time from present activity are the book presentations [17] and [18], the latter, alas, in German, albeit published in Poland. Reference [19] keeps alive the memory of Lamb's elegant solution for half-plane diffraction in parabolic coordinates. His exquisitely concise analysis for the special case of perpendicular incidence upon a half plane is presented in [20]. In [21] one finds a lively discussion of parabolic coordinates applied to diffraction, effectively illustrated and containing once more a robust bibliography to related work by Lamb, Credeli, Epstein, and even by Poincare. Reference [21] is but one example in a tutorial archive embracing an absolutely phenomenal cornucopia of physical topics.

Treatments of half-plane, $\gamma = 2\pi$ diffraction via the Wiener-Hopf method run legion. They are evolved along a traditional, integral-equation route in [8] (*Chapter V. Diffraction by a Plane Screen*), then almost exclusively via the so-called Jones method in [10] and [22]. The Jones method, in a nutshell, simply sidesteps from the very outset a cumbersome integral-equation intermediary by subjecting to Fourier transformation and boundary matching all underlying differential equations. A fully explicit Wiener-Hopf diffractive solution in a traditional context, of considerable pedagogical value, is on offer in [23].

An alternative to the Wiener-Hopf technique in the form of dual integral equations set amid a plane wave context has been evolved by P. C. Clemmow and is elaborated in [13]. A collateral presentation by him of similar material is found in the form of a collaborative contribution to [24]. In [25] a brisk, Wiener-Hopf solution of the Sommerfeld diffraction problem provides a subordinate backdrop for comparison against Clemmow's dual integral equation method. Reference [26] discusses at length sound pulse diffraction by a hard wedge, a substantially more intricate phenomenon than the pure time-harmonic scattering/diffraction entertained all along.

A fresh impetus was imparted to wedge diffraction theory by the work of G. D. Maliuzhinets, who was able to generalize the Sommerfeld formalism so as to cope with surface boundary conditions more general than those of the present perfectly conducting default. Moreover, the Maliuzhinets apparatus has some overlap with the Kontrorovich-Lebedev (K-L) transform, and with the work of T. B. A. Senior. The original K-L/Maliuzhinets sources, alas, remained largely entombed throughout the second half of the last century in Russian language tomes, and were thus difficult to acquire [27], while the anglophone literature was quite reticent in the matter of the K-L transform, the single available reference being [28], and that, too, in exceedingly scarce supply. It is most fortunate indeed that explicit use of the K-L transform can nevertheless be found in papers of high elegance, [29] and [30], which, while couched in the arena of electrostatics, offer nonetheless a sound tutorial basis for application to the time-harmonic fields presently of interest.¶¶ The Maliuzhinets/K-L wedge analysis fervor remains undiminished. Indeed, the 1995 IEEE Antennas and Propagation Symposium devoted *two* sessions to wedge scattering alone [31, 32], and there appeared recently a systematic monograph [33] which renders these methods available to a wide audience.

Extensions and refinements of the Wiener-Hopf method advance at a furious pace in the explosive work of Vito Daniele and Guido Lombardi in Turin, Italy, among several others, filling in every analytic nook of wedge theory, penetrable or not. Reference [34], an adequate sample, sets the tone and high

---

¶¶ The qualifier *harmonic* in the title of [30] alludes merely to Laplace's equation, and has no connection with time *per se*.

quality of these efforts, which are given further voice as a chorus of both theory and myriad applications in the monograph [35], a sister in some sense to [33].

Still other references may be cited in support of the (null interior)/(self-consistent interior) field emphasis, references that provide elegant alternatives to contrast against the heavy labor incurred along traditional boundary matching lines. Although these are not addressed to wedge diffraction *per se*, they do underscore the benefits, both theoretical and numerical, that naturally accrue from basing one's arguments on field shielding/field self-consistency.

REFERENCES

1. Grzesik, J., "Field matching through volume suppression," *IEE Proceedings, Part H (Antennas and Optics)*, Vol. 127, No. 1, 20–26, Feb. 1980.

2. Sommerfeld, A., "Mathematische theorie der diffraction," *Mathematische Annalen*, Vol. 16, 317–374, 1896.

3. MacDonald, H. M., "Appendix D," *Electric Waves*, 186–198, Cambridge University Press, Cambridge, UK, 1902.

4. Sommerfeld, A., P. Frank, and R. von Mises, eds., "Theorie der Beugung," *Die Differential- und Integralgleichungen der Mechanik und Physik, Zweiter physikalische teil*, Chap. 20, 808–830, Friedrich Vieweg & Sohn, Braunchshweig, Deutschland, 1935 (Mary S. Rosenberg, WWII publisher, New York, NY, USA, 1943).

5. Sommerfeld, A., *Optics, Lectures on Theoretical Physics*, Vol. IV, 249–272, Academic Press, New York, NY, USA, Translated from the German by O. Laporte and P. A. Moldauer, 1954.

6. Pauli, W., "On asymptotic series for functions in the theory of diffraction of light," *Phys. Rev.*, Vol. 54, 924–931, Dec. 1, 1938.

7. Landau L. D. and E. M. Lifshitz, "Electrodynamics of continuous media," *Course of Theoretical Physics*, Vol. 8, 304–312, Addison-Wesley Publishing Company, Reading, Mass., USA, Translated from the Russian by J. B. Sykes and J. S. Bell, 1960.

8. Baker, B. B. and E. T. Copson, "Sommerfeld's theory of diffraction," and "Diffraction by a plane screen," *The Mathematical Theory of Huygens Principle*, 2nd Edition, Chap. 4, 124–152, and Chap. 5, 153–189, Clarendon Press, Oxford, UK, 1949.

9. Stratton, J. A., *Electromagnetic Theory*, 364–369, McGraw-Hill Book Company, New York, NY, USA, 1941.

10. Mittra, R. and S. W. Lee, *Analytical Techniques in the Theory of Guided Waves*, (preferred Riemann sheet) 20–23, (Wiener-Hopf) 82ff, (Jones method) 97ff, The MacMillan Company, New York, NY, USA, 1971.

11. Watson, G. N., *A Treatise on the Theory of Bessel Functions*, 2nd Edition, (formulae (2) and (3)) 405, Cambridge University Press, Cambridge, UK, 1966.

12. Clemmow, P. C., "Some extensions of the method of steepest descents," *QJMAM*, Vol. 3, No. 2, 924–931, 1950.

13. Clemmow, P. C., *The Plane Wave Spectrum Representation of Electromagnetic Fields*, 43–58, (with particular attention to 56–58), IEEE, Inc., New York, NY, USA, 1996.

14. Ciarkowski, A., J. Boersma, and R. Mittra, "Plane-wave diffraction by a wedge — A spectral domain approach," *IEEE Trans. Antennas Propag.*, Vol. 32, No. 1, 20–29, Jan. 1, 1984.

15. Hacivelioğliu, F., L. Sevgi, and P. Y. Ufimtsev, "Electromagnetic wave scattering from a wedge with perfectly reflecting boundaries: Analysis of asymptotic techniques," *IEEE Antennas Propag. Mag.*, Vol. 53, No. 3, 232–253, Jun. 2011.

16. Ufimtsev, P. Y., *Fundamentals of the Physical Theory of Diffraction*, John Wiley and Sons, Inc., Hoboken, NJ, USA, 2007.

17. Bateman, H., "Diffraction problems," *Partial Differential Equations of Mathematical Physics*, Chap. 11, 476–490, Dover Publications, New York, NY, USA, 1959.

18. Rubinowicz, A., "Beugung an einer Halbebene," *Die Beugungswelle in der Kirchhoffschen Theorie der Beugung*, Chap. 4, 125–149, Panstwowe Wydawnictwo Naukowe, Warsaw, Poland, 1957.

19. Lamb, H., "On Sommerfeld's diffraction problem, and on reflection by a parabolic mirror," *Proc. London Math. Soc.*, Vol. 4, 190ff, 1906.

20. Lamb, S. H., *Hydrodynamics*, 6th Edition, Sec. 308, 538–541, Dover Publications, New York, NY, USA, 1945.

21. MacDonald, K. T., "Sommerfeld's diffraction problem," *Physics Examples*, 1–18, Dept. of Physics, Princeton University, Princeton, NJ, USA, Jun. 25, 2014.

22. Noble, B., *Methods Based on the Wiener-Hopf Technique*, Pergamon Press, New York, NY, USA, 1958.

23. Schwinger, J., L. L. DeRaad, Jr., K. A. Milton, and W.-Y. Tsai, "Exact solution for current," *Classical Electrodynamics*, Sec. 48, 512–516, Perseus Books, Reading, Mass., USA, 1998.

24. Born, M. and E. Wolf, "Rigorous diffraction theory," *Principles of Optics*, 7th (expanded) Edition, Chap. 11 (contributed by P. C. Clemmow), 633–672, Cambridge University Press, Cambridge, UK, 2003.

25. Carrier, G. F., M. Krook, and C. E. Pearson, "Dual integral equations," *Functions of a Complex Variable*, Sec. 8-5, 399–404, McGraw-Hill Book Company, New York, NY, USA, 1966.

26. Friedlander, F. G., "The diffraction of a pulse by a wedge," *Sound Pulses*, Chap. 5, 108–146, Cambridge University Press, Cambridge, UK, 1958.

27. Grinberg, G. A., *Selected Problems in the Mathematical Theory of Electric and Magnetic Phenomena*, Chap. 22, USSR Academy of Sciences, Moscow, 1948.

28. Sneddon, I. N., "The Kontorovich-Lebedev transform," *The Use of Integral Transforms*, Chap. 6, 353–368, McGraw-Hill Book Company, New York, NY, USA, 1972.

29. Nikoskinen, K. I. and I. V. Lindell, "Image solution for poisson's equation in wedge geometry," *IEEE Trans. Antennas Propag.*, Vol. 43, No. 2, 179–187, Feb. 1995.

30. Scharstein, R. W., "Green's function for the harmonic potential of the three-dimensional wedge transmission problem," *IEEE Trans. Antenn Propag.*, Vol. 52, No. 2, 452–460, Feb. 2004.

31. "Session 6, scattering by wedges I," *Symposium Digest, Volume Two, IEEE AP-S International Symposium and USNC/URSI National Radio Science Meeting*, 1067ff., Newport Beach, CA, USA, Jun. 18–Jun. 23, 1995.

32. "Session 9, scattering by wedges II," *Symposium Digest, Volume Two, IEEE AP-S International Symposium and USNC/URSI National Radio Science Meeting*, 1347ff., Newport Beach, CA, USA, Jun. 18–Jun. 23, 1995.

33. Lyalinov, M. A. and N. Y. Zhu, "Scattering of wedges and cones by impedance boundary conditions," *The Mario Boella Series on Electromagnetism in Information and Communication*, SciTech Publishing, The Institution of Engineering and Technology, Edison, NJ, 2013.

34. Daniele, V. G. and G. Lombardi, "Wiener-Hopf solution for impenetrable wedges at skew incidence," *IEEE Trans. Antennas Propag.*, Vol. 54, No. 9, 2472–2485, Sep. 2006.

35. Daniele, V. G. and R. S. Zich, "The Wiener-Hopf method in electromagnetics," *The Mario Boella Series on Electromagnetism in Information and Communication*, SciTech Publishing, The Institution of Engineering and Technology, Edison, NJ, 2014.